arXiv:hep-ph/0407082v1 7 Jul 2004

The static force in background perturbation theory

A.M.Badalian and A.I.Veselov
State Research Center, Institute of Theoretical and
Experimental Physics, Moscow, 117218 Russia

February 2, 2008

Abstract

The static force $F_B(r)$ and the strong coupling $\alpha_F(r)$, which defines the gluon-exchange part of $F_B(r)$, are studied in QCD background perturbation theory (BPT). In the region $r \lesssim 0.6$ fm $\alpha_F(r)$ turns out to be essentially smaller than the coupling $\alpha_B(r)$ in the static potential. For the dimensionless function $\Phi_B(r) = r^2 F_B(r)$ the characteristic values $\Phi_B(r_1) = 1.0$ and $\Phi_B(r_0) = 1.65$ are shown to be reached at the following $Q\bar{Q}$ separations: $r_1\sqrt{\sigma} = 0.77$, $r_0\sqrt{\sigma} = 1.09$ in quenched approximation and $r_1\sqrt{\sigma} = 0.72$, $r_0\sqrt{\sigma} = 1.04$ for $n_f = 3$. The numbers obtained appear to be by only 8% smaller than those calculated in lattice QCD while the values of the couplings $\alpha_F(r_1)$ and $\alpha_F(r_0)$ in BPT are by $\sim 30\%(n_f = 3)$ and $50\%(n_f = 0)$ larger than corresponding lattice couplings. With the use of the BPT potential good description of the bottomonium spectrum is obtained.

1 Introduction

The static $Q\bar{Q}$ interaction plays a special role in hadron physics and the modern understanding of the spin-independent part of the static potential $V(r)$ comes from different approaches: QCD phenomenology [1] - [3], perturbative QCD [4, 5], the analytical perturbation theory [6], the background perturbation theory (BPT) [7, 8], and lattice QCD [9]-[11]. It has been established that in the region $r \gtrsim 0.2$ fm this potential can be taken as a sum of nonperturbative (NP) confining potential plus a gluon-exchange term:

$$V(r) = V_{NP}(r) + V_{GE}(r). \tag{1}$$

Such an additive form was introduced by the Cornell group already 30 years ago, just after discovery of charmonium [1], and later it has been supported by numerous calculations in QCD phenomenology and also on

the lattice, where for the lattice potential the parametrization like the Cornell potential is used [9,10],

$$V_{lat}(r) = \sigma r - \frac{e_{lat}}{r}, \quad (r \gtrsim 0.2 \text{ fm}) \tag{2}$$

with $e_{lat} = const, \quad \alpha_{lat} = \frac{3}{4} e_{lat}$. (For the lattice static potential we use here the notation $\alpha_{lat}(e_{lat})$ to distinguish it from the phenomenological case).

In BPT the additive form (1) can automatically be obtained in the lowest approximation when both NP and Coulomb terms satisfy the Coulomb scaling law with an accuracy a few percents, in good agreement with the lattice data [12].

The explicit form of NP term is well known now: $V_{NP}(r) = \sigma r$ at the $Q\bar{Q}$ separations $r > T_g$, where T_g is the gluonic correlation length, $T_g \cong 0.2$ fm, measured on the lattice [13]. Such linear behavior is valid up to the distances $r \sim 1.0$ fm, while at larger r,due to the $q\bar{q}$–pair creation, the flattening of confining potential, is expected to take place [14]. Here in our paper we restrict our consideration to the region $r \lesssim 1.0$ fm.

Numerous calculations of the meson spectra have shown that linear potential defines gross features of the spectra, in particular, the slope and the intercept of Regge – trajectories for light mesons [15]. At the same time the splittings between low-lying levels, the fine-structure splittings, and the wave function at the origin in heavy quarkonia are shown to be very sensitive to the gluon-exchange part of the static potential (1) [2, 16]:

$$V(r) = \sigma r + V_{GE}(r), \tag{3}$$

$$V_{GE}(r) \equiv -\frac{4}{3}\frac{\alpha_{st}(r)}{r}.$$

Unfortunately, our knowledge of this term (or the vector coupling $\alpha_{st}(r)$) in IR region remains insufficient and the choice of $\alpha_{st}(r)$ essentially differs in different theoretical approaches. The only common feature of $\alpha_{st}(r)$, used in QCD phenomenology, BPT, and supported by the lattice calculations, is that this coupling freezes at large distances,

$$\alpha_{st}(\text{ large } r) = const = \alpha_{crit}. \tag{4}$$

but the true value of α_{crit} is not fixed up to now. For example, in the Cornell potential, used in the phenomenology, the typical values of the

Coulomb constant in (2) lie in the range 0.39÷0.45 [1-3,16] while on the lattice in the same parametrization (2) α_{lat} has the value by 50÷30% smaller: in quenched approximation ($n_f = 0$) $\alpha_{lat} \cong 0.20 \div 0.23$ [9]-[11] and in $(2+1)$ QCD $\alpha_{lat} \cong 0.30$ [11].

Even larger freezing value is obtained if the asymptotic freedom (AF) behavior of $\alpha_{st}(r)$ (or $\alpha_{st}(q)$ in momentum space) is taken into account. In BPT large $\alpha_{crit} = 0.58 \pm 0.02$ follows from the analysis of the splittings between low-lying levels in bottomonium [16,17] and this number is in striking agreement with α_{crit}, introduced by Godfrey, Isgur in [3] in phenomenological way. From the analysis of the hadronic decays of the τ-lepton the number $\alpha_s(1GeV) \cong 0.9 \pm 0.1$ was determined in Ref. [18], while essentially smaller value, $\alpha_s(1GeV) \cong 0.45$, was obtained in perturbative QCD with higher order corrections [19]. The Richardson potential as well as "the analytical perturbation theory" give even larger $\alpha_{crit}(n_f = 3) = 1.4$ [6]. Thus at present the true freezing value of the vector coupling, as well as α_s(1 GeV), remains unknown.

Besides the vector coupling $\alpha_{st}(r)$ (in the static potential) the coupling $\alpha_F(r)$, associated with the static force, can be introduced,

$$F(r) = V'(r) = \sigma + V'_{GE}(r), \tag{5}$$

$$V'_{GE}(r) \equiv \frac{4}{3}\frac{\alpha_F(r)}{r^2}, \tag{6}$$

where by definition $\alpha_F(r)$ is expressed through $\alpha_{st}(r)$,

$$\alpha_F(r) = \alpha_{st}(r) - r\alpha'_{st}(r). \tag{7}$$

Then an important information about the derivative $\alpha'_{st}(r)$ can be obtained from the study of the force. Note that the matrix elements over the static force define the squared wave function at the origin for the nS states in heavy quarkonia. In the lattice analysis the vector coupling α_{lat} in $V_{lat}(r)$ (2) is supposed to be independent of the $Q\bar{Q}$ separation r over the whole region 0.2 fm ÷1.0 fm [10], i.e. $\alpha'_{lat} = 0$, and therefore in this region $\alpha_{lat} \cong \alpha_F = const$. This statement is in accord with recent calculations of the lattice force in [11] where equal values $\alpha_F^{lat}(r_1) = \alpha_F^{lat}(r_0)$ at the points $r_1 \approx 0.34$ fm, $r_0 = 0.5$ fm have been obtained.

Different picture takes place in BPT where the vector coupling $\alpha_B(r)$ at the points $r_1 = 0.34$ fm and $r_0 = 0.5$ fm changes by 20% (see Section 4) being close to the freezing value only at large distances, $r \gtrsim 0.6$ fm.

Also due to the r-dependence an essential difference between $\alpha_F(r)$ and $\alpha_B(r)$ occurs just in the range $0.2\text{fm} \leq r \lesssim 0.6$ fm.

Therefore several features of the vector coupling still need to be clarified.

First, why in lattice QCD and in QCD phenomenology the Coulomb constant, used in the same Cornell potential, differs by 30% ($n_f = 3$)?

Second, whether the r-dependence of the vector coupling $\alpha_{st}(r)$ (also of $\alpha_F(r)$) really exists and why it is not observed on the lattice?

Third, what is the true freezing value?

To answer some of these questions we shall use in our analysis here BPT which gives a consistent analytical description of the vector coupling both in momentum and in coordinate spaces. To test the BPT conception about the vector-coupling behavior in the IR region, recently the heavy-quarkonia spectra have been successfully described in this approach with the use of only fundamental quantities: the current (pole) quark mass, $\Lambda_{\overline{MS}}(n_f)$, and the string tension [16],[17]. It is important that in BPT the vector coupling $\alpha_B(q)$ has correct perturbative limit at large q^2, and therefore it is fully defined by the QCD constant $\Lambda_{\overline{MS}}$ and also by so-called background mass M_B which is proportional $\sqrt{\sigma}$.

Additional information about $Q\bar{Q}$ static interaction can be extracted from the study of the static force $F_B(r)$ in BPT, with further comparison to recent lattice results from [11]. To this end it is convenient to calculate the dimentionless function $\Phi(r) = r^2 F(r)$ at two characteristic points – $r_1\sqrt{\sigma}$, $r_0\sqrt{\sigma}$, where

$$\Phi(r_1\sqrt{\sigma}) = 1.0 \quad \text{and} \quad \Phi(r_0\sqrt{\sigma}) = 1.65. \tag{8}$$

On the lattice the values $\sqrt{\sigma}r_1^{(l)}, \sqrt{\sigma}r_0^{(l)}$ are shown to be different in quenched approximation and in $(2+1)$ QCD. The same function $\Phi_B(r)$, calculated here in BPT, aquires the values (8) at the points $\sqrt{\sigma}r_1$, $\sqrt{\sigma}r_0$ which appear to be only by 8% smaller than those on the lattice. However, the freezing value α_{crit} in BPT is shown to be essentially larger than α_{lat}. To compare the BPT and the lattice potentials we calculate here the splittings between low-lying states in bottomonium and demonstrate that the lattice static potential cannot provide good agreement with experiment, while in BPT such an agreement takes place for the conventional values of the pole mass of b quark, the string tension, and $\Lambda_{\overline{MS}}(n_f = 5)$. We give also explanation why between the freezing values

in BPT and in the Cornell potential, used in phenomenology, there is the difference about 25%.

The paper is organized as follows. In Section 2 we shortly present the vector coupling in BPT and discuss the correct choice of the QCD constant Λ_V in the Vector-scheme. In Section 3 the characteristics of the lattice force are presented while in Section 4 the values $r_1\sqrt{\sigma}, r_0\sqrt{\sigma}$ are calculated in BPT. The difference between the vector couplings in both approaches is also discussed. In Section 5 the splittings between low-lying states in bottomonium are used as a test to compare the static potentials from the lattice data, in phenomenology, and in BPT. We show that the lattice static potential cannot provide good agreement with experiment. In Section 6 we present our Conclusion.

2 The strong coupling in BPT

In BPT the gluon-exchange term $V^B_{GE}(r)$ defines the vector (background) coupling $\alpha_B(r)$ in the same way, as "the exact coupling" $\alpha_{st}(r)$ is defined in Eq. (3):

$$V_B(r) = \sigma r + V^B_{GE}(r); \quad V^B_{GE}(r) = -\frac{4}{3}\frac{\alpha_B(r)}{r} \tag{9}$$

With the use of the Fourier transform of the potential $V^B_{GE}(q)$ the background coupling in coordinate space can be expressed through the coupling $\alpha_B(q)$ in momentum space [20]:

$$\alpha_B(r) = \frac{2}{\pi}\int_0^\infty \frac{dq}{q}\sin(qr)\alpha_B(q), \tag{10}$$

where the vector coupling in momentum space is defined at all momenta in Euclidean space and has no singularity for $q^2 > 0$ [7]. In two-loop approximation the coupling

$$\alpha_B(q) = \frac{4\pi}{\beta_0 t_B}\left(1 - \frac{\beta_1}{\beta_0^2}\frac{\ln t_B}{t_B}\right), \tag{11}$$

$$t_B = \ln\frac{q^2 + M_B^2}{\Lambda_V^2}, \tag{12}$$

contains the background mass M_B which enters under logarithm as a moderator of the IR behavior of the perturbative coupling. In $\alpha_B(q)$

the Landau ghost pole disappears while the short distance perturbative behavior, as well as the Casimir scaling property of the static potential, stays intact [12].

The value of M_B is determined by the lowest excitation of a hybrid [21], however this mass cannot be considered as an additional (fitting) parameter in the theory, since in QCD string theory it can be calculated on the same grounds as mesons, being expressed through the only (besides Λ_V) dimensional parameter $\sqrt{\sigma}$:

$$M_B = \xi\sqrt{\sigma} \tag{13}$$

We suppose here that in the static limit the coefficient ξ does not depend (or weakly depends) on the number of flavors n_f. Direct calculation of M_B has not yet done and therefore the number ξ has been extracted from two fits: from the comparison of lattice static potential to that in BPT [20] and from the analysis of the spectra in charmonium and bottomonium [16,17], with the following result:

$$M_B = 2.236(11)\sqrt{\sigma}. \tag{14}$$

In particular, the values $M_B = 1.0$ GeV and 0.95 GeV correspond to $\sigma = 0.20$ GeV^2 and 0.18 GeV^2.

Note that the logarithm (12) in $\alpha_B(q)$ formally coincides with that suggested in Refs. [22] many years ago in the picture where the gluon acquires an effective mass m_g and, as a result, in (11) instead of M_B^2 the value $(2m_g)^2$ enters. However, the physical gluon has no mass and in BPT the parameter M_B has been interpreted in correct way as a hybrid excitation of the $Q\bar{Q}$ string, which is proportional $\sqrt{\sigma}$ [21].

The background coupling $\alpha_B(q)$ has correct PQCD limit at $q^2 \gg M_B^2$ and therefore the constant $\Lambda_V(n_f)$ (in Vector-scheme) under the logarithm (12) can be expressed through the conventional QCD constant $\Lambda_{\overline{MS}}(n_f)$ as in PQCD [23]:

$$\Lambda_V(n_f) = \Lambda_{\overline{MS}}(n_f)\exp\left(\frac{a_1}{2\beta_0}\right) \tag{15}$$

with $a_1 = \frac{31}{3} - \frac{10}{9}n_f$, $\beta_0 = 11 - \frac{2}{3}n_f$. At present the values of $\Lambda_{\overline{MS}}^{(n_f)}$ are well established in two cases – from high-energy processes for $n_f = 5$ [24] and in quenched approximation from lattice calculations [25]:

$$\Lambda_{\overline{MS}}^{(5)}(2-loop) = (216 \pm 25)\ \text{MeV}\ , \tag{16}$$

which corresponds to the "world average" $\alpha_s(M_Z) = 0.117 \pm 0.002$, and the value

$$\Lambda^{(0)}_{\overline{MS}}(2-loop) = \frac{0.602(48)}{r_0} = (237 \pm 19) \text{ MeV} \tag{17}$$

(with $r_0 = 0.5$ fm $= 2.538$ GeV^{-1}) was calculated on the lattice in [25].

Then from (15) the corresponding values of $\Lambda_V(n_f)$ in the Vector-scheme are following,

$$\Lambda_V^{(5)} = (295 \pm 35) \text{ MeV}, \tag{18}$$

$$\Lambda_V^{(0)} = (379 \pm 30) \text{ MeV}. \tag{19}$$

It is worthwhile to notice that the background coupling $\alpha_B(r)$ (12) is a universal function of the ratio

$$\lambda(n_f) = \frac{\Lambda_V(n_f)}{M_B}, \tag{20}$$

and actually depends on the dimensionless variable $x = rM_B$ and λ:

$$\alpha_B(r, \Lambda_V, M_B) \equiv \alpha_B(rM_B; \lambda) = \frac{2}{\pi} \int \frac{dx}{x} \sin(x, rM_B)\alpha_B(x, \lambda). \tag{21}$$

The same ratio λ also defines the freezing (critical) value of the coupling (which coincides in momentum and coordinate spaces), and it is given by the analytical expression,

$$\alpha_{crit}(q \to 0) = \alpha_{crit}(r \to \infty) = \frac{4\pi}{\beta_0 t_{crit}} \left\{ 1 - \frac{\beta_1}{\beta_0^2} \frac{\ln t_{crit}}{t_{crit}} \right\}, \tag{22}$$

$$t_{crit} = \ln \frac{M_B^2}{\Lambda_V^2} = \ln \lambda^2(n_f). \tag{23}$$

Taking Λ_V from (18), (19) and M_B (14) one obtains the following numbers for α_{crit}:

in quenched approximation

$$\alpha_{crit}(n_f = 0) = 0.419 \begin{array}{l} +0.045 \\ -0.038, \end{array} \tag{24}$$

while for $n_f = 5$ the freezing value is by $\sim 30\%$ larger,

$$\alpha_{crit}(n_f = 5) = 0.510 \begin{array}{l} +0.055 \\ -0.049, \end{array} \quad (M_B = 1.0 \text{ GeV }) \tag{25}$$

and

$$\alpha_{crit}(n_f=5) = 0.533 \begin{array}{l}+0.062\\ -0.053,\end{array} \quad (M_B = 0.95 \text{ GeV }). \tag{26}$$

Note that the freezing value (26) turns out to be very close to that, phenomenologically introduced by Godfrey , Isgur in [3] to describe a lot of experimental data in meson sector. As shown in [17], the choice with $M_B = 0.95$ GeV $\Lambda_V^{(5)} \cong 320$ MeV, and $\alpha_{crit} = 0.58$, provides good agreement between experiment and BPT calculations of the splittings in bottomonium. Thus, in BPT the large freezing value $\alpha_{crit}(n_f=5) \approx 0.58$ appears to be consistent with the conventional value of $\Lambda_{\overline{MS}}^{(5)} \approx 230$ MeV, $\alpha_s(M_Z, 2-loop) = 0.119 \pm 0.001$.

However, the large freezing value in BPT (and in QCD phenomenology) does not agree with the value used in the lattice parametrization (2) of the static potential. For example, in quenched approximation $\alpha_{lat} \cong 0.23$ was obtained in [9,10], while in BPT the <u>minimal</u> value α_{crit} (which corresponds to the minimal value in (19), $\Lambda_{\overline{MS}}^{(0)}(\min) = 218$ MeV) is equal $\alpha_{crit}^{\min}(n_f=0) = 0.38$, i.e., by 40% larger. Such a difference between two numbers partly occurs due to the fact that on the lattice the r-dependence of the vector coupling is not seen (or neglected) at $r > 0.2$ fm .

In Table 1 the background coupling $\alpha_B(r)$ is compared to $\alpha_{st}^P(r)$, calculated in PQCD, where according to the perturbative prescription the QCD constant $\Lambda_R^{(n_f)}$ in coordinate space is defined as $\Lambda_R^{(n_f)} = e^\gamma \Lambda_V^{(n_f)}$ (γ is the Euler constant). These couplings (both in two-loop approximation) appear to be close to each other only at very small distances, $r < 0.1$ fm, and have the characteristic feature that the difference $\Delta\alpha = \alpha_B(r) - \alpha_{st}^P(r)$ is positive at $r \leq 0.04$ fm and becoming negative at $r > 0.04$ fm; just such a change of the sign of $\Delta\alpha$ has been observed in lattice static potential [10].

Table 1: The strong coupling $\alpha_{st}^P(2-loop, r)$ in PQCD and the background coupling $\alpha_B(2-loop, r)$ in BPT in quenched approximation with $\Lambda_{\overline{MS}}^{(0)} = 237$ MeV ($\Lambda_V^{(0)} = 379$ MeV, $\Lambda_R^{(0)} = 675$ MeV, $M_B = 1.0$ GeV)

r(fm)	$\alpha_{st}^P(r)$	$\alpha_B(r)$
0.01	0.128	0.138
0.02	0.156	0.166
0.04	0.202	0.204
0.06	0.248	0.232
0.08	0.301	0.254
0.10	0.368	0.272
0.12	0.457	0.288
0.14	0.588	0.301

3 The static force on the lattice

The study of the static force is especially convenient through the dimensionless function $\Phi_{lat}(r)$ since this function depends on the dimensionless variable like $\frac{r}{a}$, where a is a lattice spacing , or on $r\sqrt{\sigma}$ (if the string tension is taken as the only mass scale). Recently $\Phi_{lat}(r)$ was measured by the MILC group both in quenched case and in $(2+1)$ lattice QCD [11] with the following results:

First, the function $\Phi_{lat}(r) = r^2 F_{lat}(r) = (r\sqrt{\sigma})^2 F(r\sqrt{\sigma})$ acquires the value $\Phi_{lat}(r_1^l) = 1.0$ at the $Q\bar{Q}$ separation r_1^l:

$$r_1^l\sqrt{\sigma} = 0.769 \pm 0.002 \quad (n_f = 3) \tag{27}$$

$$r_1^l\sqrt{\sigma} = 0.833 \pm 0.002 \quad (n_f = 0). \tag{28}$$

Second, the function Φ_{lat} has the value $\Phi_{lat}(r_0\sqrt{\sigma}) = 1.65$ at the following separation r_0^l (the Sommer scale):

$$r_0\sqrt{\sigma} = 1.114 \pm 0.002 \quad (n_f = 3) \tag{29}$$

$$r_0\sqrt{\sigma} = 1.160 \pm 0.002 \quad (n_f = 0). \tag{30}$$

Also in [11] the ratio

$$\frac{r_0^l}{r_1^l} = 1.449(5) \quad (n_f = 3) \tag{31}$$

is defined with a precision accuracy. If in (27)-(31) one takes the string tension $\sigma = 0.20$ GeV^2, then the characteristic points are $r_1^l = 0.34$ fm,

$r_0^l = 0.49$ fm for $n_f = 3$ and slightly larger, $r_1^l = 0.37$ fm, $r_0^l = 0.51$ fm in quenched case. The numbers obtained can be used to extract the vector coupling $\alpha_F^{lat}(r)$, associated with the force in lattice QCD:

$$F_{lat}(r) = \sigma + \frac{4}{3r^2}\alpha_F^{lat}(r), \tag{32}$$

$$\Phi_{lat}(r) = \sigma r^2 + \frac{4}{3}\alpha_F^{lat}(r). \tag{33}$$

From (27)-(31) it follows that the values of $\alpha_F^{lat}(r)$ are equal at the points r_1^l and r_0^l with a good accuracy:

$$\alpha_F^{lat}(r_1^{(l)}) = \alpha_F^{lat}(r_0^{(l)}) = 0.307(4) \quad (n_f = 3), \tag{34}$$

$$\alpha_F^{lat}(r_1^{(l)}) = \alpha_F^{lat}(r_0^{(l)}) = 0.229(3) \quad (n_f = 0). \tag{35}$$

Note that in quenched case the value (35) for $\alpha_F^{lat}(r)$ numerically coincides with the lattice coupling $\alpha_{lat} = 0.23$ in the static potential (where $\alpha_{lat} = const$ is assumed over the whole region 0.2 fm $\leq r \lesssim 1.0$ fm). Thus existing lattice data are consistent with the assumption that the derivative in this region is equal zero, $\alpha'_{lat}(r) = 0$.

The lattice number (34) in full QCD appears to be essentially smaller than the coupling, used in BPT and also in QCD phenomenology, in IR region. In order to make a conclusion, which value provides better description of experimental data, in Section 5 as a test we shall calculate the bottomonium spectrum with the lattice as well as with the BPT static potentials.

4 The static force in BPT

In BPT the static force can be presented as in (5),

$$F_B(r) = \sigma + \frac{4}{3r^2}\alpha_F(r), \tag{36}$$

where the coupling $\alpha_F(r)$, associated with the force $F_B(r)$, can be expressed through the known coupling $\alpha_B(r)$ (10) and its derivative:

$$\alpha_F(r) = \alpha_B(r) - r\alpha'_B(r). \tag{37}$$

Correspondingly, the dimensionless function $\Phi_B(r)$ is

$$\Phi_B(r) = r^2 F_B(r) = (\sqrt{\sigma} r)^2 + \frac{4}{3}\alpha_F(r). \tag{38}$$

The coupling $\alpha_F(r)$ can be easily calculated from the expression (10) and due to negative contribution of the term with the derivative it appears to be essentially smaller than $\alpha_B(r)$ (in the region $r \lesssim 0.6$ fm). The values of $\alpha_F(r)$ for $n_f = 0$ and $n_f = 3$ are given in Tables 2,3, from which the r-dependence of $\alpha_F(r)$ is explicitly seen:

i) At the distances $r = 0.2$ fm; 0.35 fm, and 0.50 fm the coupling $\alpha_F(r)(n_f = 3)$ is smaller than $\alpha_B(r)$ (in the static potential) by 25%, 18%, and 12%, respectively.

ii) The derivative $\alpha'_B(r)$ is larger for larger n_f being approximately proportional β_0^{-1} ($\beta_0 = 11 - \frac{2}{3}n_f$).

iii) At the distance $r \approx 0.2$ fm the coupling $\alpha_F(r, n_f)$ in BPT coincides with α_{lat} both for $n_f = 3$ and $n_f = 0$ but at larger $r > 0.2$ fm it manifests essential growth: for $n_f = 3$ $\alpha_F(r = 0.335$ fm$)$ =0.376, $\alpha_F(r_0 = 0.493$ fm$)$ =0.430, being by $\sim 20\%$ and $\sim 40\%$ larger than $\alpha_{lat} = 0.306$ from [11].

Table 2: The background couplings $\alpha_F(r) = \alpha_B(r) - r\alpha'_B(r)$ and $\alpha_B(r)$ in quenched approximation ($\Lambda_V^{(0)} = 379$ MeV, $M_B = 1.0$ GeV, $\alpha_{crit} = 0.419$)

r(fm)	$\alpha_F(r)$	$\alpha_B(r)$	r(fm)	$\alpha_F(r)$	$\alpha_B(r)$
0.099	0.188	0.272	0.355	0.312	0.379
0.118	0.201	0.289	0.394	0.324	0.386
0.138	0.213	0.301	0.433	0.335	0.391
0.158	0.225	0.313	0.473	0.345	0.396
0.197	0.246	0.333	0.493	0.350	0.398
0.236	0.265	0.348	0.532	0.358	0.401
0.296	0.290	0.365	0.591	0.369	0.406
0.335	0.305	0.375	α_{crtit}	0.419	0.419

Table 3: The background couplings $\alpha_F(r) = \alpha_B(r) - r\alpha'_B(r)$ and $\alpha_B(r)$ for $n_f = 3$ ($\Lambda_V^{(3)} = 370$ MeV, $M_B = 1.0$ GeV, $\alpha_{crit} = 0.510$)

r(fm)	$\alpha_F(r)$	$\alpha_B(r)$	r(fm)	$\alpha_F(r)$	$\alpha_B(r)$
0.099	0.233	0.336	0.355	0.385	0.464
0.118	0.250	0.355	0.394	0.399	0.472
0.138	0.265	0.371	0.433	0.413	0.478
0.158	0.279	0.385	0.473	0.425	0.484
0.197	0.305	0.409	0.493	0.430	0.486
0.236	0.328	0.427	0.512	0.435	0.488
0.296	0.358	0.448	0.532	0.440	0.490
0.335	0.376	0.459	0.591	0.453	0.495

Knowing $\alpha_F(r)$ the function $\Phi_B(r)$ (38) can be easily calculated. Note that the coupling $\alpha_F(r)$ (as well as $\alpha_B(r)$) weakly depends on the string tension through the background mass $M_B = 2.236\sqrt{\sigma}$ (16). We have obtained the following numbers for the separations r_1 and r_0, where $\Phi_B(r_1) = 1.0$ and $\Phi_B(r_0) = 1.65$:

$$\begin{aligned} r_1\sqrt{\sigma} &= 0.769(5) \qquad (n_f = 0) \\ r_0\sqrt{\sigma} &= 1.090(5), \end{aligned} \tag{39}$$

and the ratio r_0/r_1 coincides with $r_0^{(l)}/r_1^{(l)}(n_f = 0)$ on the lattice with 2% accuracy:

$$\frac{r_0}{r_1} = 1.417(16)(n_f = 0).$$

For $n_f = 3$ in BPT the characteristic separations are following,

$$\begin{aligned} r_1\sqrt{\sigma} &= 0.716(4) \\ r_0\sqrt{\sigma} &= 1.044\ (5) \qquad (n_f = 3) \\ \frac{r_1}{r_0} &= 1.458(15) \end{aligned} \tag{40}$$

The comparison of obtained numbers to those in lattice QCD shows that $r_1\sqrt{\sigma}(r_0\sqrt{\sigma})$ in BPT is only by 8% (6%) smaller than the lattice values (27)-(30) while the ratio r_1/r_0 in (40) coincides with (31) with 1% accuracy.

To have a full picture – how the separations $r_1\sqrt{\sigma}, r_0\sqrt{\sigma}$ are changing with a increase of flavors, below we give their values also for $n_f = 5$ (see Table 4):

$$\begin{aligned} \sqrt{\sigma}r_1 &= 0.673(4), \qquad (n_f = 5) \\ \sqrt{\sigma}r_0 &= 1.016(5), \end{aligned} \tag{41}$$

with their ratio

$$\frac{r_0}{r_1} = 1.510(16) \quad (n_f = 5).$$

Table 4: The background couplings $\alpha_B(r)$ and $\alpha_F(r)$ for $n_f = 5$ ($\Lambda_V^{(5)} = 320$ MeV, $M_B = 1.0$ GeV, $\alpha_{crit} = 0.548$)

r(fm)	$\alpha_F(r)$	$\alpha_B(r)$	r(fm)	$\alpha_F(r)$	$\alpha_B(r)$
0.099	0.274	0.381	0.355	0.435	0.508
0.118	0.292	0.401	0.394	0.450	0.515
0.138	0.309	0.417	0.433	0.463	0.521
0.158	0.324	0.432	0.473	0.474	0.526
0.197	0.352	0.455	0.493	0.479	0.528
0.236	0.377	0.473	0.512	0.484	0.530
0.296	0.409	0.494	0.532	0.488	0.532
0.335	0.427	0.504	0.591	0.501	0.536

Comparing (39)-(41) one can see the points $r_1(n_f), r_0(n_f)$ are smaller for larger n_f (for $n_f = 5$ they are by 12% smaller than in quenched case). Also for $n_f = 5$ the coupling $\alpha_F(r)$ approaches a freezing value at smaller distances, e.g. the value $\alpha_F(r_0)/\alpha_{crit}$ is equal 0.835 ($n_f = 0$), 0.843 ($n_f = 3$), 0.874 ($n_f = 5$). (See also Fig.1.)

In contrast to lattice coupling $\alpha_F^{lat}(r)$, which is supposed to be r–independent between r_1 and r_0, (34, 35), in BPT the coupling $\alpha_F(r)$ depends on r and calculated values of $\alpha_F(r_1)$, $\alpha_F(r_0)$ are given below:

$$\begin{aligned} \alpha_F(r_1^{(0)}\sqrt{\sigma}) &= 0.306 \quad (n_f = 0), \\ \alpha_F(r_1^{(3)}\sqrt{\sigma}) &= 0.366 \quad (n_f = 3), \\ \alpha_F(r_1^{(5)}\sqrt{\sigma}) &= 0.412 \quad (n_f = 5), \end{aligned} \tag{42}$$

and at the Sommer scale $r_0\sqrt{\sigma}$ their values are by $\sim 12\%$ larger,

$$\begin{aligned} \alpha_F(r_0^{(0)}\sqrt{\sigma}) &= 0.346 \quad (n_f = 0), \\ \alpha_F(r_0^{(3)}\sqrt{\sigma}) &= 0.42 \quad (n_f = 3), \\ \alpha_F(r_0^{(5)}\sqrt{\sigma}) &= 0.46 \quad (n_f = 5). \end{aligned} \tag{43}$$

From our analysis one can conclude that

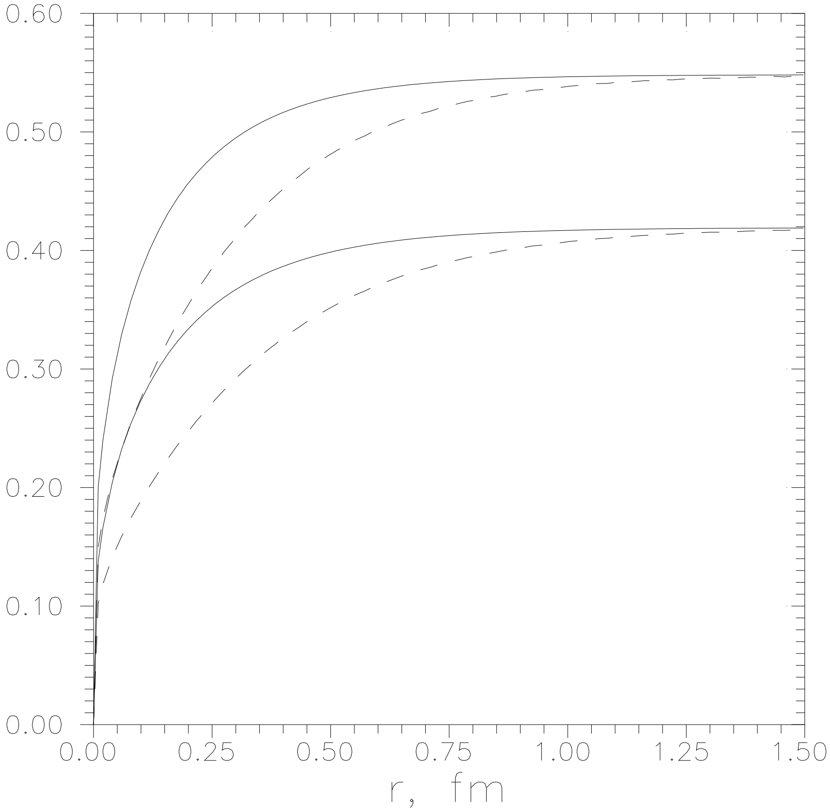

Figure 1: The couplings $\alpha_B(r)$ solid lines) and $\alpha_F(r)$ (dashed lines). The upper curves refer to case with $n_f = 5$ and the lower curves refer to quenched case ($n_f = 0$).

i) The characteristic quantities $r_1\sqrt{\sigma}, r_0\sqrt{\sigma}$ in BPT are very close to the corresponding lattice values being only by 8% smaller.

ii) At the same time the coupling $\alpha_F(r_0)$ in the "background force" $F_B(r)$ is shown to be by 30%-40% larger than α_F^{lat}.

5 The $b\bar{b}$ spectrum as a test of the vector coupling in IR region

Recently it was demonstrated that the bottomonium spectrum, especially the splittings between low-lying levels, appear to be very sensitive both to the freezing value and to the r-dependence of the vector coupling [16,17]. Therefore just these splittings can be used for testing of $\alpha_{st}(r)$ in IR region. For illustration we consider here three typical static potentials.

First one imitates the lattice static potential (2) but has the form of the Cornell potential over the whole region $r \geq 0$. The coupling $\alpha_{lat}(r) = const = 0.306$ is taken from lattice calculations with $n_f = 3$

from [11] which is the largest Coulomb constant obtained in lattice measurements up to now. In this potential the AF behavior of $\alpha_{lat}(r)$ (which was observed on the lattice at small $Q\bar{Q}$ separations, $r \lesssim 0.2$ fm [9]) is neglected and therefore such the gluon-exchange potential with $\alpha_{lat} = const$ over the whole region is stronger than the lattice potential and gives rise to larger values of the splittings between levels in bottomonium.

Second variant refers to the phenomenological Cornell potential with $\alpha_{st}(r) = const = 0.42$ which is used in analysis of charmonium [1,26].

Third potential is taken as in BPT for $n_f = 5$, $\Lambda_V^{(5)} = 330$ MeV (or $\Lambda_{\overline{MS}}^{(5)}(2-\text{loop}) = 241$ MeV), and $M_B = 0.95$ GeV. The calculations with first two potentials are performed with nonrelativistic kinematics while for third potential the solutions of relativistic Salpeter equation are used.

The splittings between the spin-averaged masses $\bar{M}(nL)$ in bottomonium for these three potentials are given in Table 5.

Table 5: The splittings (in MeV) between spin averaged masses in bottomonium for the Cornell potential with (A) $\alpha_{lat} = 0.306; (B)\alpha_{phen} = 0.42$ and for the BPT potential with $\Lambda_V^{(5)} = 330$ MeV ($M_B = 0.95$ GeV)

Splitt.	A. $\alpha_{lat} = 0.306$ $\sigma_A = 0.20$ GeV^2 $m_A = 4.85$ GeV	B. $\alpha_{phen} = 0.42$ $\sigma = 0.183$ GeV^2 $m_B = 4.631$ GeV	C. $\alpha_{crit} = 0.565$ $\sigma = 0.178$ GeV^2 $m_b = 4.828$ GeV	exper.
2S-1S	527	615	557	$563^{a)}$
2S-1P	114	97	123	$123^{a)}$
1P-1S	413	517	434	$440^{a)}$
1D-1P	241	260	260	$261\pm2^{b)}$
2P-1P	359	368	370	360.1 ± 1.2

$^{a)}$ Since the mass of $\eta_b(nS)$ is unknown and in any case $\bar{M}(1S) < M(\Upsilon(1S))$, we give here only the low limit of the experimental splitting.

$^{b)}$ The experimental number for $M(1\text{D}_2) = 10161.2 \pm 2.2$ is obtained in [27].

From our calculations presented in Table 5 one can make important conclusions. First, the calculations with "the lattice" potential A with

$\alpha_{lat} = 0.306(n_f = 3)$ define the upper bounds of the splittings between different states in bottomonium (since the AF behavior at $r \leq 0.2$ fm is neglected). Nevertheless even upper bounds of the 2S-1S, 1P-1S splittings appear to be by 40÷30 MeV smaller than the experimental numbers (for which we know the lower bounds since the $\eta_b(nS)$ mesons are still unobserved, $\bar{M}(nS) < M(\Upsilon(nS))$).

It is of a special importance to compare theoretical and experimental number for the 1D-1P splitting which is measured now with precision accuracy [28]:

$$\Delta(\exp) = \bar{M}(1\mathrm{D}) - \bar{M}(1\mathrm{P}) = 261.1 \pm 2.2(\exp) \pm \begin{array}{c} 1.0 \\ 0.0 \end{array} (th) \text{ MeV}, \quad (44)$$

where $\bar{M}(1\mathrm{P})$ =9900.1±0.6 MeV, $\bar{M}(1\mathrm{D})$= $M_{\exp}(1\mathrm{D}_2) \pm \begin{array}{c} 1.0 \\ 0.0 \end{array} (th)$ MeV; $M_{\exp}(1\mathrm{D}_2) = 10161.2 \pm 1.6(\exp)$ MeV (see a discussion of the 1D -1P splitting in [17]).

For "the lattice" potential A the upper limit $\Delta(lat)$ turns out to be by 20 MeV smaller than $\Delta(\exp)$ (the difference is about ten standard deviations).

On the contrary the calculations with the phenomenological potential B (with $\alpha_{phen} = 0.42$) and with the BPT potential C give the precision agreement with $\Delta(\exp)$.

In BPT the 2S-1S, 1P-1S splittings are also close to the experimental numbers being only by $\sim$ 10 MeV smaller (the ground state mass $\bar{M}(1\mathrm{S})$=9466 MeV is slightly larger than expected experimental number). The same splittings for the Cornell potential ($\alpha_{phen} = const = 0.42$) turn to be too large (since $\bar{M}(1\mathrm{S}) \cong 9300$ MeV is small) because the Coulomb part of the static potential is overestimated if the AF behavior of the vector coupling is neglected. This AF effect is small for the 1D-1P splitting for which agreement with experiment takes place.

Note that in the BPT potential C the freezing value $\alpha_{crit} = 0.565$ is essentially larger than $\alpha_{phen} = 0.42$ and to understand what kind of the approximation corresponds to $\alpha_{st}(r) = const$, let us introduce an effective coupling in BPT according to the relation:

$$\langle \frac{\alpha_B(r)}{r} \rangle_{nL} = \alpha_{eff}(nL) \langle \frac{1}{r} \rangle_{nL} \quad (45)$$

Our calculations of the matrix elements demonstrate (see Table 6) that

(1) α_{eff} depends on the quantum numbers n, L;

(2) the values of $\alpha_{eff}(nL)$ appear to be by 30÷15% smaller than the freezing value $\alpha_{crit} = 0.565$ and those values for the 1S, 2S states are close to α_{phen} used in phenomenology.

Table 6: The effective vector coupling $\alpha_{eff}(nL)$ for the BPT potential C $(\Lambda_V^{(5)} = 330$ MeV, $M_B = 0.95$ GeV, $\sigma = 0.178$ GeV^2, $\alpha_{crit} = 0.565)$

state	1S	2S	3S	1P	1P	1D	2D
$\alpha_{eff}(nL)$	0.405	0.439	0.448	0.495	0.501	0.528	0.528

(3) For the orbital excitations the effective coupling $\alpha_{eff} \cong 0.50$ is by $\sim$ 20% larger than for the 1S, 2S states and just this fact results in increasing of the splittings like 2S-1P, 1D-1P which is observed in bottomonium.

To make a decisive conclusion about the behavior of $\alpha_{st}(r)$ in IR region it would be also important to take into account a screening of the gluon-exchange potential at large distances. At present there is no a theory of this phenomenon on the fundamental level, although in some cases the Coulomb screening is introduced in a phenomenological way [29].

6 Conclusion

Our study of the vector couplings $\alpha_B(r)$ (in the static potential) and $\alpha_F(r)$ in the static force $F(r)$ is performed in the framework of BPT with the following results.

Due to the derivative term $\alpha'_B(r)$ an essential difference between $\alpha_F(r)$ and $\alpha_B(r)$ is observed at the $Q\bar{Q}$ separations $r \lesssim 0.6$ fm with $\alpha_F(r)$ being by 50%, 30%, 15% smaller at the points 0.2 fm, 0.3 fm, and 0.5 fm, respectively.

At the same time the freezing values of both couplings coincide and are rather large: $\alpha_{crit} \cong 0.41(n_f = 0)$; 0.51 $(n_f = 3)$, and $\alpha_{crit} = 0.58 \pm 0.04$ for $n_f = 5$. The last number turns out to be very close to that introduced by Godfrey, Isgur in their phenomenological analysis.

The dimensionless quantities $r_1\sqrt{\sigma}$ and $r_0\sqrt{\sigma}$, where the function $\Phi(r) = r^2F(r)$ has the values 1.0 and 1.65, are calculated in BPT and

their values are by (6÷8)% smaller that those calculated on the lattice in quenched case and in (2+1) QCD.

In contrast to lattice observation where $\alpha_F^{lat}(r_1) = \alpha_F^{lat}(r_0) = const$ and this constant is small: $\alpha_{lat} = 0.23(n_f = 0)$ and $\alpha_{lat} = 0.306(n_f = 3)$, in BPT $\alpha_F(r)$ at these points is found to be by 40% larger for $n_f = 0$ and by 30% larger for $n_f = 3$. Because the Coulomb constant in the lattice static potential is small, this potential gives essentially smaller 2S-1S, 1P-1S, 1D-1P splittings in bottomonium.

The meaning of the Coulomb constant α_{phen}, used in phenomenology, as an effective coupling in BPT is suggested. This interpretation explains why $\alpha_{phen} \cong 0.42$ is by 30% smaller than the freezing value $\alpha_{crit} \cong 0.56$ for the potentials with the AF taken into account.

The knowledge of the static force in BPT is important to perform precision calculations of the wave functions at the origin, hadronic decays, and fine structure splitting in bottomonium.

7 Acknowledgement

For many years the authors have had remarkable opportunity to discuss a lot of problems in hadron physics with Prof.Simonov. His scope and the attitude in physics had an enourmous influence on us. We appreciate very much our collaboration with Yu.A.Simonov and his permanent support in our research activity.

This work was partly supported by PRF grant for leading scientific schools No 1774.2003.2 .

References

[1] E.Eichten *et al.*, Phys. Rev. Lett **34**, 369 (1975);
E.Eichten *et al.*, Phys. Rev. Lett D **21**, 203 (1980);
E.J.Eichten, K.Lane, and C.Quigg, Phys. Rev. D **89**, 162002 (2002) and references therein.

[2] D.P.Stanley and D.Robson, Phys. Rev. D **21**, 3180 (1980); Phys. Rev. Lett **45**, 325 (1980);
W.Buchmuller and S.Tye, Phys. Rev. D **24**, 132 (1981);
W.Kwong, J.L.Rosner, and C.Quigg, Ann. Rev. Nucl. Part. Sci. **37**, 325 (1987);
D.Ebert, R.N.Faustov, and V.O.Galkin, Phys. Rev D **62**, 034014 (2000).

[3] S.Godfrey and N.Isgur, Phys. Rev. D **32**, 189 (1985);
L.P.Fulcher, Phys. Rev. D **44**, 2079 (1991);
S.Jacobs, M.G.Olsson, and C.Suchyta, Phys. Rev. D **33**, 3338 (1986);
T.Y.Allen, M.G.Olsson, and S.Veseli, Phys. Rev. D **62**, 094021 (2000).

[4] A.Pineda and F.J.Yndurain, Phys. Rev. D **58**, 094022 (1998) and references therein.

[5] Y.J.Ng, Y.Pantaleone, and S.H.H.Tye, Phys. Rev. D **33**, 777(1986);
S.Recksiegel and Y.Sumino, Phys. Rev. **D67**, 014004 (2003) and references therein;
A.S.Mattingly and and P.M.Stevenson, Phys. Rev. D **49**, 437 (1994).

[6] D.V.Shirkov and I.L.Solotsov, Phys. Rev. Lett. **79**, 1209 (1997); Phys. Lett. B **442**, 344 (1998).

[7] Yu.A.Simonov, Yad. Fiz. **65**, 140 (2002); ibid. **58**, 113 (1995);
Pis'ma Zh. Eksp. Teor. Fiz. **57**, 513 (1993).

[8] Yu.A.Simonov, in *Proceedings of the XVII International School on QCD: "Perturbative or Nonperturbative",* Lisbon, 1999, Ed. by L.S.Ferreira *et al.* (World Sci., Singapore, 1999), p.60.

[9] S.P.Booth *et al.*, Phys. Lett. B **294**, 385 (1992);
G.S.Bali and K.Schilling, Phys. Rev. D **47**, 661 (1993);
G.S.Bali, Phys. Rept. **343**, 1 (2001) and references therein.

[10] G.S.Bali, Phys. Lett. B **460**, 170 (1999).

[11] MILC collaboration (C.W.Bernard *et al.*), Phys. Rev D **64**, 054506 (2001); ibid. D **62**, 034503 (2000);
A.S.Kronfeld, hep-lat/0310063.

[12] G.S.Bali, Phys. Rev. D **62**, 114503 (2000);
V.I.Shevchenko and Yu.A.Simonov, Phys. Rev. Lett. **85**, 1811 (2000); Int. J. Mod., A **18**, 127 (2003);
Yu.A.Simonov, JETP Lett. **71**, 127 (2000).

[13] A.Di Giacomo, H.G.Dosch, V.I.Shevchenko and Yu.A.Simonov, Phys. Rept. **372**, 319 (2002) and references therein.

[14] A.Duncan, E.Eichten, and H.Tacker, Phys. Rev. D **63**, 111501 (2001);B.Bolder *et al.*, Phys. Rev. D **63**, 074504 (2001);
C.Bernard *et al.*, Phys. Rev. D **64**, 074509 (2001).

[15] A.M.Badalian and B.L.G.Bakker, Phys. Rev. D **66**, 034025 (2002).

[16] A.M.Badalian and B.L.G.Bakker, hep-ph/0311010 (to be published in Yad. Fiz.).

[17] A.M.Badalian, B.L.G.Bakker, and A.I.Veselov, hep-ph/0311009, Phys. Rev. D (to be published).

[18] S.J.Brodsky *et al.*, Phys. Rev. D **67**, 055008 (2003).

[19] A.A.Pivovarov hep-ph/0301074, talk at Int. Seminar "Quarks – 2002", Novgorod, Russia, 1-7 June (2002).

[20] A.M.Badalian, Yad. Fiz. **63**, 2269 (2000);
A.M.Badalian and D.S.Kuzmenko, Phys. Rev. D **65**, 016004 (2002).

[21] A.M.Badalian and Yu.A.Simonov, Phys. Atom. Nucl. **60**, 630 (1997).

[22] Yu.A.Simonov, *"Lectures Notes in Physics"*, Vol. **479** p. 138 (Springer-Verlag, New-York, Berlin, 1996).

[23] G.Parisi and R.Petronzio, Phys. Lett. B **94**, 51 (1980);
J.M.Cornwall, Phys. Rev. D **26**, 1453 (1982).

[24] A.Billore, Phys. Lett. B **92**, 343 (11980);
M.Peter, Nucl. Phys. B **501**, 471 (1997);
Y.Schröder, Phys. Lett. B **447**, 321 (1999).

[25] Particle Data Group, Phys. Rev. D **66**, 89 (2002).

[26] S.Capitani, M.Lüscher, R.Sommer, and H.Witting, Nucl. Phys. B **544**, 669 (1999).

[27] A.M.Badalian and B.L.G.Bakker, Phys. Rev. D **67**, 071903 (2003);
A.M.Badalian and V.L.Morgunov, Phys. Rev. D **60**, 116008 (1999).

[28] CLEO Collaboration (G.Bonvicini *et al.*), hep-ex/0404021;
(S.E.Csorna *et al.*), hep-ex/0207060;
T.Skwarnicki, Int. J. Mod. Phys. A **19**, 1030 (2004).

[29] T.A.Lahde and D.O.Riska, Nucl. Phys. A **A707**, 425 (2002);
C.Semay and B.Silvester-Brac, Phys. Rev. D **52**, 6553 (1995);
Y.Vijande, P.Gonzalez, H.Carcilaro, A.Valcarce, Phys. Rev. D **69**, 074019 (2004).